Contents lists available at Science-Gate

International Journal of Advanced and Applied Sciences

Journal homepage: http://www.science-gate.com/IJAAS.html

Bioconvective variable viscosity flow of Carreau nanofluid with external heat source and nonlinear radiation: Analysis with convective heat and mass constraints

Rajab Alsayegh *

Department of Mechanical Engineering, Faculty of Engineering, King Abdulaziz University, Jeddah, Saudi Arabia

ARTICLE INFO

Article history:
Received 29 February 2024
Received in revised form
10 July 2024
Accepted 20 July 2024

Keywords:
Carreau nanofluid
Magneto-porosity
Heat transfer
Nonlinear analysis
Thermal conductivity

ABSTRACT

In this study, an unsteady model for Carreau nanofluid with microorganism decomposition is developed. The viscosity and thermal conductivity of the Carreau nanofluid are considered variable. Magnetic and porosity effects are included using a magneto-porosity parameter. An additional heat source is introduced to improve heat transfer. Nonlinear analysis is applied for radiative applications. The flow is modeled using an oscillatory stretching surface. Convective mass and heat constraints are used to analyze the problem. Analytical computations are performed on the developed model. The significance of various parameters for the thermal problem is discussed. The results may enhance the performance of transport problems, heat transmission, energy systems, and thermal devices.

1. Introduction

Driven by advances in nanotechnology, researchers have argued for the integration of nanoscale solid particles into heating and cooling mechanisms as a new energy source. Thanks to their superior thermal efficiency, these nanomaterials are recognized as an optimal thermal energy source. The impact of nanomaterials on thermal performance has made significant contributions in various sectors, including industrial manufacturing, heating appliances, nuclear power, chemical engineering, healthcare, and automobile engines. A review of the literature reveals various studies that highlight the benefits of nanofluids, enhanced by additional thermal sources and innovative designs. Javaid et al. (2022) presented the Burgers nanofluid analysis in the annulus region. Hosseinzadeh et al. (2023) described the role of nanofluid in enhancing the impact of the heat transfer phenomenon. Sheikholeslami et al. (2023) utilized solar applications based on the nanofluid flow within a porous sink surface. Shamshuddin et al. (2023) described the sensor plate flow subject to nanofluid interaction. Jalili et al. (2023) examined the Hall outcomes for nanofluid in an analytical way. The power law nanofluid with gold metallic particles was analyzed with optimized impact in the investigation of Sharma et al. (2023a). Gangadhar et al. (2024) evaluated the squeezing analysis for nanofluid in radiated surfaces. Mebarek-Oudina and Chabani (2023) analyzed the thermal energy performances utilized by nanoparticles with PCM applications. Rafique et al. (2023) discussed the slip role in fluctuated viscosity nanofluid flow containing hybrid particles. Dharmaiah et al. (2023) analyzed the nanofluid with Howarth's wavy path along with activation energy. Sharma et al. (2023b) described the micropolar nanofluid analysis for Bayesian flow. Eid et al. (2023) inspected the Dufour analysis against the uniformly driven flow of nanofluid on an inclined surface. Bhatti et al. (2023) examined the Darcy- Forchheimer aspect due to nanofluid-driven flow analytically. Khan and Shehzad (2020) utilized the Carreau nanofluid with variable thermal conductivity assessment due to moving periodic surfaces.

The phenomenon of bioconvection refers to the coordinated movement of microorganisms in a fluid triggered by a variety of environmental factors. This process involves the complex interaction of nanofluids with gyrotactic microorganisms, which underlies the functionality of the bioconvection framework. Bioconvection has diverse applications in the fields of biotechnology and environmental sciences. It allows the suspension of bacteria and other microorganisms within nanoparticles, facilitating their use in biofuel development,

* Corresponding Author.
Email Address: ralsayegh@kau.edu.sa
https://doi.org/10.21833/ijaas.2024.08.003
Corresponding author's ORCID profile:
https://orcid.org/0000-0001-9940-9110

environmental monitoring, and fertilizers, among other applications. Additionally, bioconvection holds significant importance in chemical engineering and biotechnology, introducing innovative approaches to these disciplines. Mabood et al. (2023) predicted the bioconvective enrollment for nanofluid with impressive heat transfer performances. Li et al. (2023a) utilized the pattern for bioconvection due to the melting heat nanofluid problem. Khan et al. (2023) discussed the analysis of microorganisms suspended in nanofluid under an optimized pattern. Patil et al. (2023) described the wedge flow of nanofluid with bioconvective judgment. Ghachem et al. (2023) analyzed the numerical treatment for the bioconvective-supported nanofluid problem. A study performed by Jabeen et al. (2024) explained the microorganism's role in the stability of nanofluid. Haq et al. (2023) evaluated the rotating flow with bioconvective analysis endorsed by Sutterby nanofluid. Hussain et al. (2023) predicted the 3D analysis for bioconvective nanofluid in Williamson fluid. Li et al. (2023b) directed the entropy phenomenon for Carreau nanofluid in the presence of bioconvection impact. The lubricated surface bioconvective analysis for nanofluid was utilized by Maatoug et al. (2023). Anjum et al. (2023) expressed the cross-nanofluid transport with gyrotactic microorganisms and activation energy. Ahmed et al. (2023) described the bioconvective investigation while treating the thermal properties of nanofluid. The Keller Box simulations for nanofluid with gyrotactic microorganisms were claimed by Abbas et al. (2023).

This investigation deals with the assessment of bioconvective patterns for Carreau nanofluid with variable viscosity. The combined features of magnetic force and porous medium have been entertained. The assumptions for heat transfer are directed by variable thermal conductivity. Nonlinear radiated impact and external heat transfer effects are accounted. The problem is subject to convective mass and thermal constraints. After developing the model, the simulations are performed using the homotopy analysis method (HAM). The physical dynamic of the problem is addressed.

2. Statement of problem

An incompressible Carreau nanofluid flow under the decomposition of microorganisms has been investigated. The periodically accelerating porous surface accounting the flow. The microorganisms' suspensions are utilized. The role of variable thermal conductivity and viscosity is taken into account. The additional outcomes for heat transfer are regarded by heat source. The impact of nonlinear radiation is taken into account. The magnetic force acts along normal directions. The 2D flow problem is established in the coordinate system with horizontal velocity u and normal velocity v. Such constraints lead to the following set of equations (Khan and Shehzad, 2020; Mabood et al., 2023):

$$\frac{\partial u}{\partial x}+\frac{\partial v}{\partial y}=0, \tag{1}$$

$$\frac{\partial u}{\partial t}+u\frac{\partial u}{\partial x}+v\frac{\partial u}{\partial y}=\frac{1}{\rho_f}\frac{\partial}{\partial y}\left(\mu_f(T)\frac{\partial u}{\partial y}\right)+ \nu_f\frac{3(n-1)}{2}{\lambda_*}^2\frac{\partial^2 u}{\partial y^2}\left(\frac{\partial u}{\partial y}\right)^2-\frac{\sigma B_0^2}{\rho_f}u-\frac{\nu\varphi}{k^*}u, \tag{2}$$

$$\frac{\partial T}{\partial t}+u\frac{\partial T}{\partial x}+v\frac{\partial T}{\partial y}=\frac{1}{\rho c_p}\frac{\partial}{\partial y}\left(k(T)\frac{\partial T}{\partial y}\right)+\frac{16\sigma^*}{3k^*(\rho c_p)_f}\frac{\partial}{\partial y}\left\{T^3\frac{\partial T}{\partial y}\right\}+ \frac{q^*}{(\rho c_p)_f}\left(T_f-T_\infty\right)+\Upsilon_e\left\{\begin{matrix} and D_B\frac{\partial T}{\partial y}\frac{\partial C}{\partial y} \\ and+\frac{D_T}{T_\infty}\left(\frac{\partial T}{\partial y}\right)^2\end{matrix}\right\}, \tag{3}$$

$$\frac{\partial C}{\partial t}+u\frac{\partial C}{\partial x}+v\frac{\partial C}{\partial y}=D_B\frac{\partial^2 C}{\partial y^2}+\frac{D_T}{T_\infty}\frac{\partial^2 T}{\partial y^2}-k_c\left(C_f-C_\infty\right), \tag{4}$$

$$\frac{\partial n}{\partial t}+u\frac{\partial n}{\partial x}+v\frac{\partial n}{\partial y}+\frac{b_l w_l}{(C_w-C_\infty)}\left[\frac{\partial}{\partial y}\left(n\frac{\partial C}{\partial y}\right)\right]=D_m\left(\frac{\partial^2 n}{\partial y^2}\right). \tag{5}$$

Important physical quantities are time-constant λ_*, fluid density ρ_f, electrical conductivity σ, time t, external heat source coefficient q^*, porous medium ϕ, permeability medium k^*, temperature T, variable thermal conductivity $k(T)$, Stefan Boltzmann σ, Rosseland mean absorption k^*, Brownian diffusion D_B, thermo-diffusion D_T, ambient temperature T_∞, free stream concentration C_∞, effective heat transfer ratio between particles to fluid Υ_e, reaction rate κ, chemotaxis constant b_l and swimming cells' speed w_l. The following assumptions are used for variable viscosity; the Reynolds exponential theory is used as:

$$\mu_f(\theta)=e^{-(A\theta)}=1-(A\theta)+O(A^2), \tag{6}$$

with A (viscosity coefficient).

The following assumptions are used for variable thermal conductivity:

$$k(T)=k_\infty\left[1+\delta\frac{(T_f-T_\infty)}{\Delta T}\right], \tag{7}$$

where, ambient conductivity is defined by k_∞ while δ explain the variable thermal conductivity coefficient.

The problem is incorporated with the following boundary constraints (Khan and Shehzad, 2020; Mabood et al., 2023):

$$\left.\begin{matrix} u=u_\omega=bx\sin\lambda t,\ v=0,-k\frac{\partial T}{\partial y}=h_1\left(T_f-T\right) \\ -D_B\frac{\partial C}{\partial y}=h_2\left(C_f-C\right),n=n_w\ \ at\ \ y=0,\ t>0\end{matrix}\right\} \tag{8}$$

$$u\to 0,\quad T\to T_\infty, C\to C_\infty, n\to n_\infty\ at\quad y\to\infty \tag{9}$$

where, λ defining the accelerating frequency, h_1 be heat transfer coefficient and h_2 represent the mass transfer coefficient.

The problem is entertained in view of the following variables (Khan and Shehzad, 2020):

$$\xi=\sqrt{\frac{b}{\nu}}y,\quad \tau=t\Omega_s,\quad u=bxf_y(\xi,\tau),\quad v=-\sqrt{\nu b}f(\xi,\tau), \theta(\xi,\tau)=\frac{T-T_\infty}{T_f-T_\infty},\phi(\xi,\tau)=\frac{C-C_\infty}{C_f-C_\infty},\chi(\xi,\tau)=\frac{n-n_\infty}{n_w-n_\infty}. \tag{10}$$

The new arranged system is:

$$(1-A\theta)f_{\xi\xi\xi}-Sf_{\xi\tau}-f_\xi^2+ff_{\xi\xi}+\frac{3(n-1)We}{2}f_{\xi\xi}f_{\xi\xi}^2- Haf_\xi=0, \tag{11}$$

$\frac{1}{Pr}[1+\epsilon\theta+\frac{4}{3}Rd\{1+(\theta_f-1)\theta\}^3]\theta_{\xi\xi}+\frac{1}{Pr}[\epsilon+4Rd(\theta_f-1)(1+(\theta_f-1)\theta)^2](\theta_\xi)^2+f\phi_\xi+Nb\theta_\xi\phi_\xi+Nt(\theta_\xi)^2-S\theta_\tau+Q\theta=0$ (12)

$\varphi_{\xi\xi}+\frac{Nt}{Nb}\theta_{\xi\xi}-S(Sc)\varphi_\tau+Scf\varphi_\xi-(Sc)kr\varphi=0,$ (13)

$\chi_{\xi\xi}-S(Lb)\chi_\tau+Lb\chi_\xi-Pe[\varphi_{\eta\eta}(\chi+\Lambda_g)+\chi_\xi\varphi_\eta]=0.$ (14)

Subjecting to dimensionless constraints:

$f_\xi(0,\tau)=\sin\tau,\ f(0,\tau)=0,\ \theta_\xi(0,\tau)=-\gamma_1[1-\theta(0,\tau)],\phi_\xi(0,\tau)=-\gamma_2[1-\phi(0,\tau)],\chi(0,\tau)=1,$ (15)

$f_\xi(\infty,\tau)\to 0,\theta(\infty,\tau)\to 0,\varphi(\infty,\tau)\to 0,\chi(\infty,\tau)\to 0$ (16)

where, We is the Carreau fluid parameter, the magneto-porosity parameter, β is the magneto-porosity constant, θ_f is surface heating constant, $\gamma_2$the concentration Biot number, S is oscillation frequency to stretched rate ratio, Q_f is the heat generation/absorption coefficient, Rd is the radiation parameter, Nb is the Brownian parameter, Pe is the Peclet number, Nt is the thermophoresis constant, Λ_g represents the microorganisms' concentration fluctuation, γ_1 is the thermal Biot number and Lbbioconvection Lewis number having the following relations:

$We=\lambda_*{}^2b^2x^2/\nu_f,\quad \beta=\frac{\sigma B_0^2}{b\rho_f}+\frac{\nu\varphi}{bk^*},\quad S=\Omega_s/b,\quad Rd=4\sigma^*T_\infty{}^3/3k^*k_\infty,\quad \theta_f=T_f/T_\infty,\quad Nb=\Upsilon_eD_B(C_f-C_\infty)/\nu_f,\quad Nt=\Upsilon_eD_T(T_f-T_\infty)/T_\infty\nu_f,\quad Q_f=q^*/b(\rho c_p)_f,\quad \Lambda_g=n_\infty/(n_w-n_\infty),\quad Pe=b_lw_l/D_m,\quad Lb=\nu_f/D_m,\gamma_1=(h_1/k)\sqrt{\nu_f/b},\gamma_2=(h_2/D_m)\sqrt{\nu_f/b}.$

Defining the local Nusselt number, local Sherwood number, and motile density number (Shamshuddin et al., 2023; Mabood et al., 2023):

$\frac{Nu}{\sqrt{Re_x}}=-\left(1+\frac{4}{3}Rd\theta_w^3(0,\tau)\right),\frac{Su}{\sqrt{Re_x}}=-\varphi_\xi(0,\tau),\frac{Nn}{\sqrt{Re_x}}=-\chi_\xi(0,\tau).$ (17)

3. Analytical scheme

The main problem involves complex partial differential equations (PDEs), making it challenging to compute a solution. The solution is developed using the HAM, which is preferred due to its high accuracy. To begin the simulations, we first select an initial guess:

$f_0(\xi,\tau)=\sin\tau\left(1-e^{-\xi}\right),\theta_0(\xi)=e^{-\xi},\varphi_0(\xi)=e^{-\xi},\chi_0(\xi)=e^{-\xi}.$ (18)

With auxiliary linear operators

$\pounds_f=\frac{\partial^3}{\partial\xi^3}-\frac{\partial}{\partial\xi},\pounds_\theta=\frac{\partial^2}{\partial\xi^2}-1,\pounds_\varphi=\frac{\partial^2}{\partial\xi^2}-1,\pounds_\chi=\frac{\partial^2}{\partial\xi^2}-1$ (20)

with solution:

$\pounds_f\left(\sum_{r=0}^{2}\omega_{r+1}e^{(r-1)\xi}\right)=0,$ (21)

$\pounds_\theta\left(\sum_{r=3}^{4}\omega_{r+1}e^{(-1)^r\xi}\right)=0,$ (22)

$\pounds_\varphi\left(\sum_{r=5}^{6}\omega_{r+1}e^{(-1)^r\xi}\right)=0,$ (23)

$\pounds_\phi\left(\sum_{r=7}^{8}\omega_{r+1}e^{(-1)^r\xi}\right)=0,$ (23)

where, $\Psi_j(j=1,2,\ldots,9)$ are unknown constants.

4. Convergence analysis

The desirable accuracy obtained via HAM is based on values of auxiliary coefficients. These auxiliary coefficients h_f,h_θ h_ϕ and h_χ play a vital role in ensuring the convergence region. The illustration of these parameters is achieved by plotting h –curve in Fig. 1. For an admissible range of parameters, the numerical values can be chosen from $-1.6\le h_f\le -0.1$, $-1.9\le h_\theta\le 0.1$, $-1.7\le h_\phi\le -0.2$ and $-1.8\le h_\chi\le 0$.

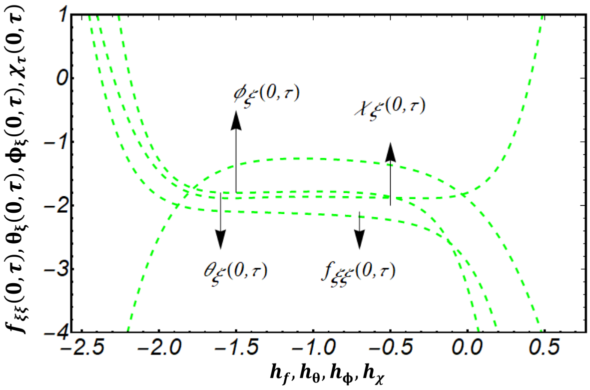

Fig. 1: $h-$ curves for $f_{\xi\xi},\theta_\xi,\varphi_\xi$ and χ_ξ

5. Numerical model verification

Before analyzing the physical aspects of the problem, the computed results are verified first. Table 1 presents the accuracy of simulated results compared to the findings of Abbas et al. (2008) and Zheng et al. (2023) with the variation of τ. A good concordance between the results is noticed.

Table 1: Comparison of $f_{\xi\xi}(0,\tau)$ with Abbas et al. (2008) and Zheng et al. (2013) when $A=0,S=n=1,M=12$

τ	Abbas et al. (2008)	Zheng et al. (2023)	Present results
1.5π	11.678656	11.678656	11.678656
5.5π	11.678707	11.678706	11.678706
9.5π	11.678656	11.678656	11.678656

6. Results and discussion

Fig. 2a presents the change of velocity f_ξ with time τ for various Carreau fluid coefficients We. An increasing amplifying of velocity with oscillatory behavior is observed. The oscillatory nature of f_ξ is exhibited due to the sinusoidal motion of velocity. The Weissenberg number is a dimensionless number that describes the ratio of elastic to viscous forces in a fluid flow. It is often used in the study of non-Newtonian fluids, where the fluid's viscosity can change with the flow conditions. In Fig. 2a, as We increases, the amplitude of the oscillations seems to decrease slightly, and the waveform appears to become less sinusoidal and more complex. This implies that higher elastic effects (higher We) dampen the oscillatory behavior of f_ξ.

Fig. 2b identifies the outcomes of magneto-porosity parameter β on judgement of f_ξ. A reducing oscillation is preserved for f_ξ in view of larger β. Basically, β summarizing the joint role of magnetic force and porous media. For higher values of β, the peaks and troughs of the waveform are slightly more pronounced, suggesting that β amplifies the characteristics of the oscillations. The magnetic force contributes to the Lorentz force, while the effects of porous media are explained by the permeability of the porous region. Both forces significantly reduce the velocity. Fig. 2c comprises the assessment for f_ξ in view of variable viscosity coefficient A. Slower velocity with declining amplitude is exhibited for an increase in A.

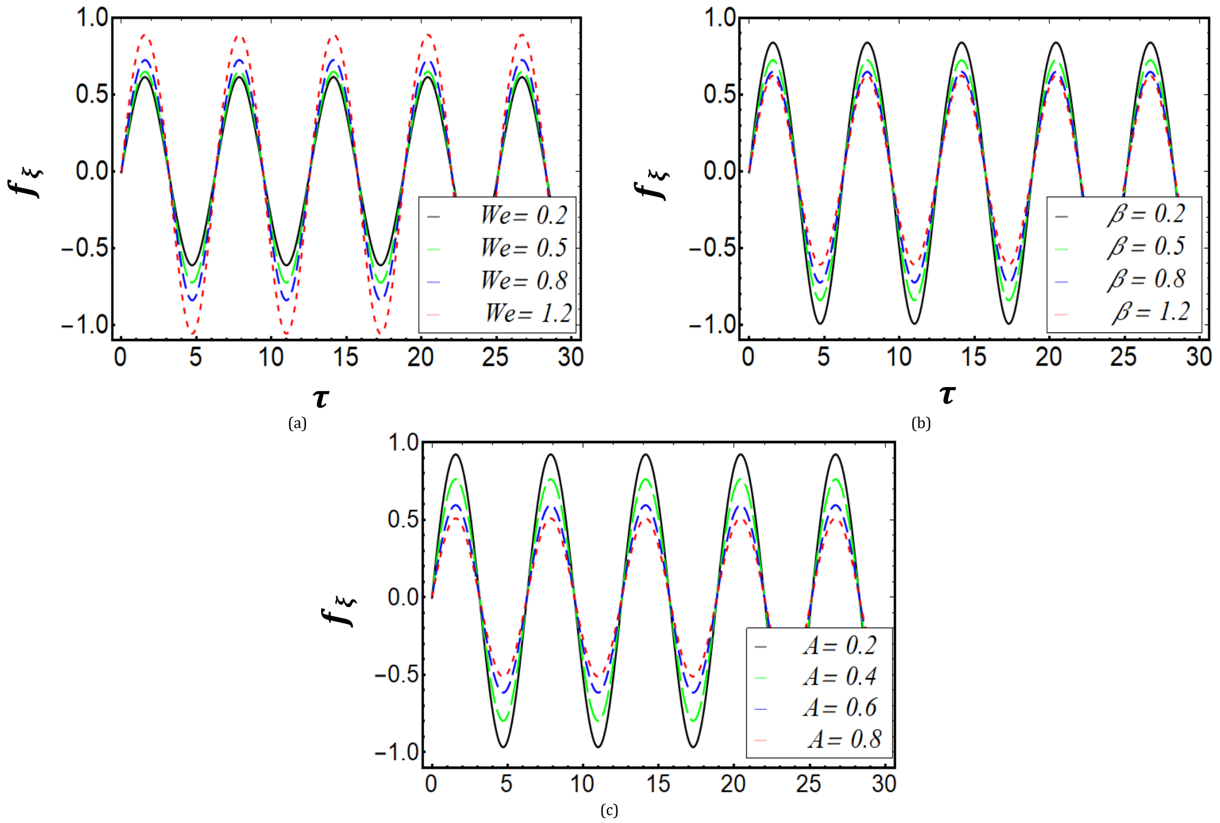

Fig. 2: Effects of (a) We (b) β (c) A on the temporal variation of f_ξ

Fig. 3a illustrates an analysis of the temperature profile θ due to larger variable viscosity parameter A. shows an increase in the temperature profile θ as A increases. This is due to the temperature-dependent viscosity, and as viscosity changes, it affects the thermal energy distribution. The onset of the Carreau fluid coefficient We on temperature field θ has been evaluated in Fig. 3b. The decrement is noted in the evaluation of θ due to We. The decrement in θ with increasing We suggests that elastic forces in the fluid act to decrease the temperature profile, which is due to a change in the internal fluid motion that reduces thermal energy distribution. Fig. 3c justifies the determined role of magneto-porosity parameter β on θ. The enhanced truncation in θ with justified range of β has been exhibited. Physically, β attributes both magnetic force and porous medium applications which enhance the thermal phenomenon. The observed truncation in θ with an increase in β indicates that magnetic forces and the porosity of the medium affect the convection and conduction processes by altering the flow paths and enhancing thermal dissipation. Fig. 3d contributes the role of variable thermal conductivity constant δ on θ. The variable assumptions for thermal conductivity leading to improvement in θ. In different energy systems, the thermal conductivity of involved materials cannot be treated as a constant. The interpretation that variable thermal conductivity leads to an improvement in θ aligns with the concept that a material's ability to conduct heat can vary with temperature, and accounting for this variability can lead to a more accurate description of the thermal profile.

Fig. 4a claims the truncation in temperature field θ by contributing the effective role of surface heating parameter θ_f. The association of θ_f is associated to nonlinear radiated phenomenon. With increasing θ_f, temperature get enlarging. The investigation performed in Fig. 4b aims to involve the effects of external heat source parameter Q_f on θ. The contribution of Q_f present external heat source to moving surface, which enhances the rate of temperature within fluid particles. Fig. 4c analyzes the significance of thermal Biot number h_1 on θ. A raise in θ subject to h_1 is noticed. Physically, h_1 accounting the effective features of the heat transfer coefficient due to which θ get boosted. Fig. 4d shows an increasing enrollment in pattern of θ due to thermophoresis parameter Nt. Such outcomes are due to thermos-diffusion phenomenon.

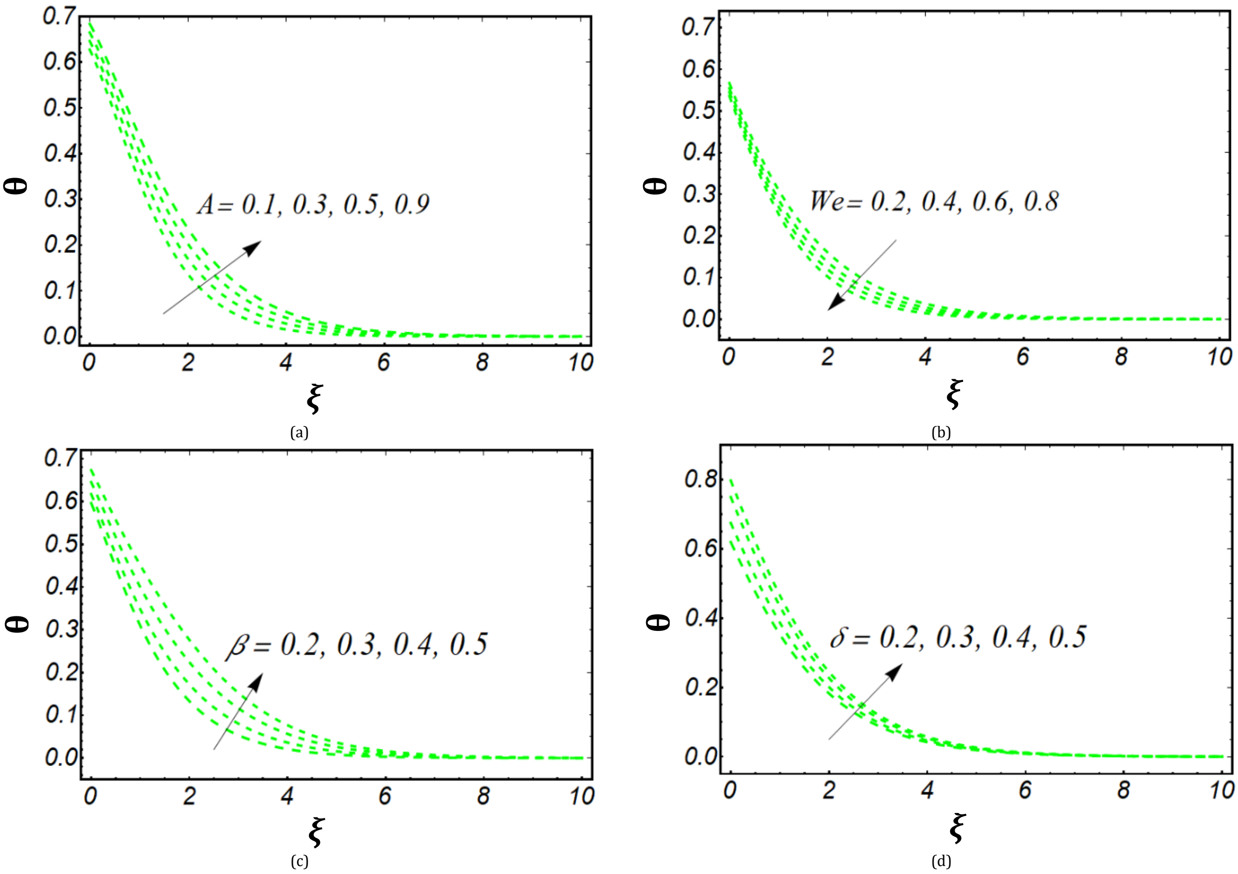

Fig. 3: Effects of (a) A (b) We (c) β (d) δ on the temperature profile

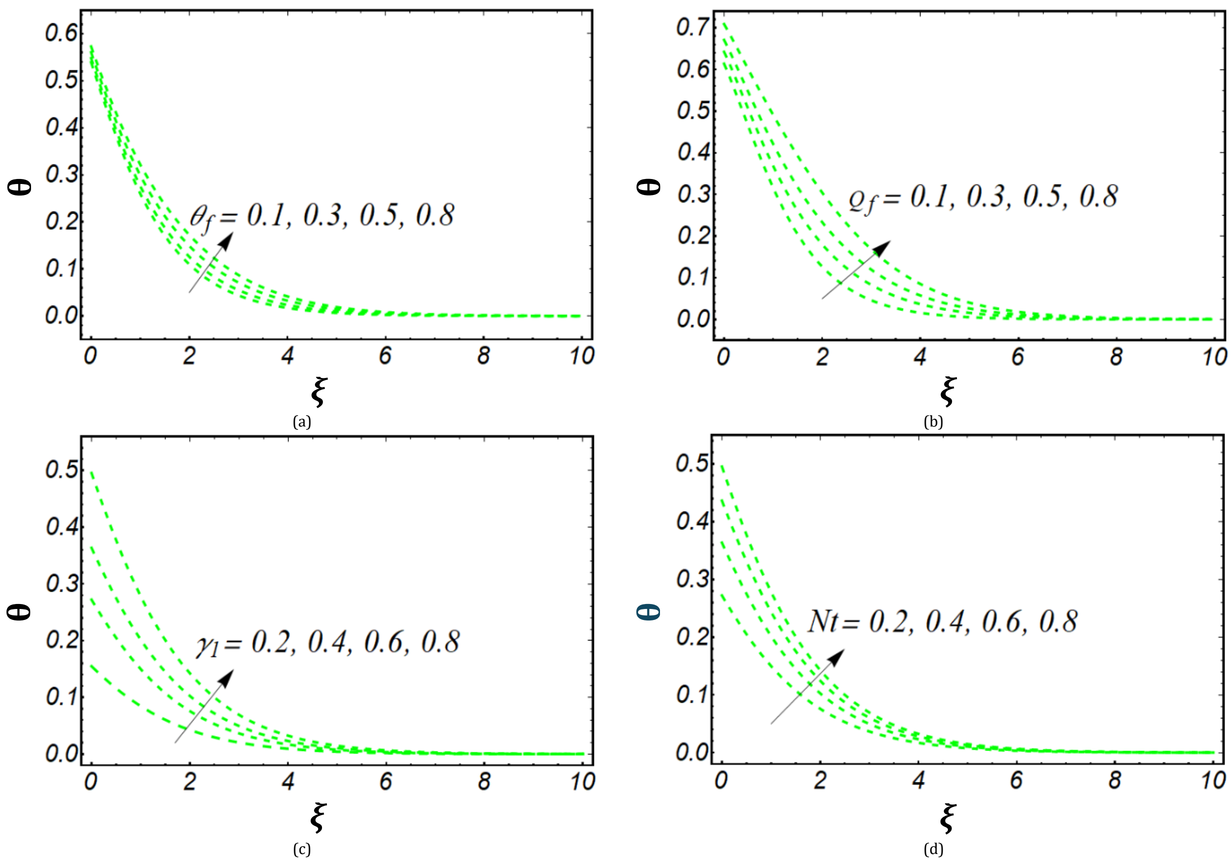

Fig. 4: Effects of (a) θ_f (b) Q_f (c) γ_1 (d) Nt on the temperature profile

Fig. 5a discusses the truncated profile of concentration ϕ due to concentration Biot number γ_2. Upshot observations are evaluated in the assessment of ϕ due to γ_2. Due larger γ_2, the mass transfer coefficient enhances. Fig. 5b determines the outcomes for Schmidt number Sc on ϕ. Declining effects of Sc are noticed on ϕ. Such decreasing outcomes due to low mass diffusivity. Fig. 5c addresses the analysis for ϕ by varying variable viscosity coefficient A. Enhancement is predicted for ϕ against A. Fig. 5d presents the analysis for We on ϕ. Lower changes in ϕ due to We are claimed. Fig. 5e announces the concentration of nanofluid decomposition decreases when the chemical reaction parameter gets kr varied.

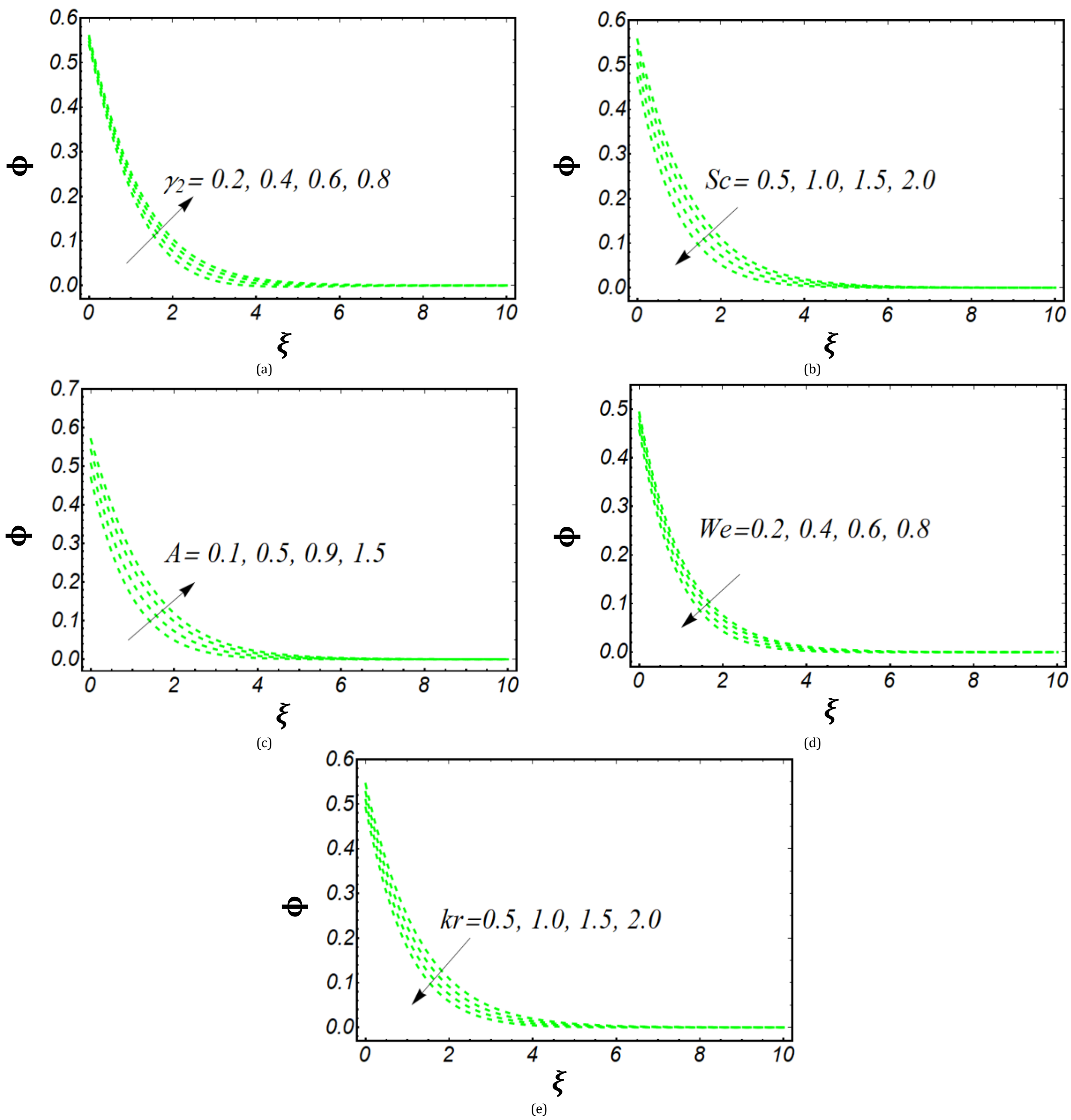

Fig. 5: Effect of (a) γ_2 (b) Sc (c) A (d) We (e) kr on the concentration profile

Fig. 6a reports that interaction for microorganisms' profile χ subject to We. The microorganisms profile showing reducing prediction due to We. Fig. 6b addresses the continuation of Peclet number Pe on χ. Reducing change in χ is exhibited for variation of Pe. Less motile diffusivity is involved for enlarging Pe which turn down the assessment of χ. Same observations are exhibited for bioconvective Lewis number in Fig. 6c. Table 2 presents the numerical impact of different parameters on $-\theta_\xi(0,\tau), -\phi_\xi(0,\tau)$ and $-\chi_\xi(0,\tau)$. An increase in We leads to a steeper negative gradient, which suggests that elastic effects are enhancing heat transfer. Similar to θ, ϕ also shows a more negative gradient with increasing We, indicating a stronger rate of decrease in concentration due to the enhanced mixing. As with θ and ϕ , a larger We results in a larger negative gradient for microorganism concentration, implying that elasticity is dispersing the microorganisms more effectively. The temperature gradient decreases as β increases, which indicates that magnetic forces and porosity impede the transfer of heat, by altering flow patterns. The gradient of ϕ also decreases with β, suggesting that the diffusion and advection of the chemical species is being moderated.

The microorganism concentration gradient shows a decrease with higher β, due to the magnetic field's alignment effects or the porous medium's filtration effects. A varying S affects the temperature gradient, suggesting that unsteady flow is impacting thermal transfer rates. Changes in S affect ϕ's gradient, which implies that unsteady flow affects the dispersion of nanoparticles. The gradient of χ changes with S, indicating that flow unsteadiness effectively disperses the microorganisms. Higher A values show a more negative temperature gradient, suggesting that variable viscosity enhances the heat transfer. A similar trend is observed for ϕ, indicating that the concentration of the nanoparticles decreases more rapidly with variable viscosity.

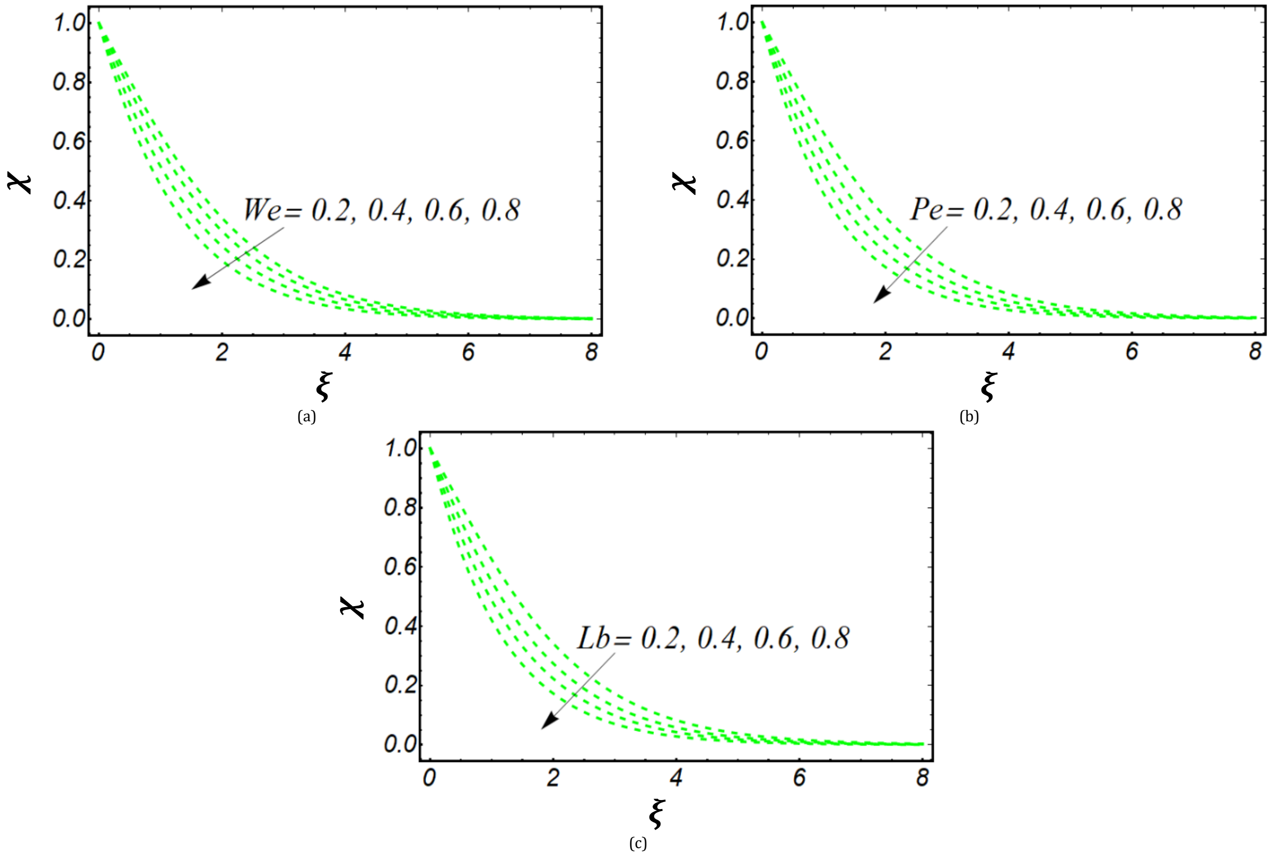

Fig. 6: Effects of (a) We (b) Pe (c) Lb on the microorganism's profile

Table 2: Numerical impact of the governing parameters on $-\theta_\xi(0,\tau)$, $-\phi_\xi(0,\tau)$ and $-\chi_\xi(0,\tau)$

We	β	S	Pr	Nb	A	δ	$-\theta_\xi(0,\tau)$	$-\phi_\xi(0,\tau)$	$-\chi_\xi(0,\tau)$
0.2	0.1	0.5	0.3	0.3	0.7	0.5	0.84357	0.66365	0.54320
0.4							0.86851	0.69748	0.57784
0.8							0.91478	0.73012	0.61297
0.3	0.4						0.81254	0.67789	0.57754
	0.6						0.76021	0.64320	0.54751
	1.0						0.73785	0.62785	0.51325
		0.2					0.76965	0.64624	0.59781
		0.4					0.72789	0.62389	0.51329
		0.8					0.68365	0.58145	0.47625
			0.4				0.79785	0.65751	0.54751
			1.0				0.83778	0.67017	0.58325
			1.4				0.87325	0.71754	0.63145
				0.2			0.75785	0.64632	0.52320
				0.4			0.7445	0.61145	0.47965
				0.6			0.71896	0.57785	0.45857
					0.4		0.74325	0.67554	0.56021
					0.8		0.72034	0.64789	0.53324
					1.2		0.67780	0.58215	0.51785
						0.4	0.79447	0.62785	0.54715
						1.0	0.83320	0.66532	0.57750
						1.6	0.84497	0.69785	0.59302

The trend is consistent for microorganism concentration as well, with variable viscosity potentially causing a more rapid decrease in concentration. The gradient of temperature seems to be affected by δ, indicating that the temperature profile is sensitive to changes in thermal conductivity. The gradient of ϕ shows variability with δ, suggesting an interaction between thermal properties and chemical dispersion. The microorganism concentration gradient also changes with δ, which means that thermal conductivity indirectly affects microorganism distribution.

7. Conclusions

In this study, a dynamic model is presented for the Carreau nanofluid that incorporates the decomposition of microorganisms. The viscosity and thermal conductivity of the Carreau nanofluid are considered to vary. The effects of magnetism and porosity are integrated via the magneto-porosity parameter. Additionally, the introduction of extra heat sources aims to improve the heat transfer issue. A nonlinear approach is adopted for applications involving radiation. An oscillating stretching surface facilitates the promotion of flow. The examination of the issue employs convective mass and heat restrictions. Analytical methods are applied to tackle the formulated problem. The main results can be summarized as follows:

- The velocity profile of the nanofluid is enhanced when larger numerical values are assigned to the Carreau fluid parameter.
- A minimal numerical impact on the velocity profile is observed with the viscosity parameter.
- Heat transfer is significantly increased by the magneto-porosity parameter and the surface heating parameter.
- The addition of an extra heat source effectively boosts the temperature profile.
- As the thermal Biot number increases, so does the temperature profile.
- The concentration profile decreases with the Carreau fluid parameter and the chemical reaction constant.
- An improving trend in the concentration profile is observed with the concentration Biot number.
- Both the Nusselt number and the Sherwood number are reduced by the magneto-porosity parameter.

Compliance with ethical standards

Conflict of interest

The author(s) declared no potential conflicts of interest with respect to the research, authorship, and/or publication of this article.

References

Abbas T, Al-Khaled K, Raza AH, Ayadi M, Chammam W, and Khan SU (2023). Inclined magnetized flow of radioactive nanoparticles with exponential heat source and slip effects: Keller box simulations. Journal of Nanofluids, 12(2): 571-579. https://doi.org/10.1166/jon.2023.1935

Abbas Z, Wang Y, Hayat T, and Oberlack M (2008). Hydromagnetic flow in a viscoelastic fluid due to the oscillatory stretching surface. International Journal of Non-Linear Mechanics, 43(8): 783-793. https://doi.org/10.1016/j.ijnonlinmec.2008.04.009

Ahmed J, Nazir F, Fadhl BM, Makhdoum BM, Mahmoud Z, Mohamed A, and Khan I (2023). Magneto-bioconvection flow of Casson nanofluid configured by a rotating disk in the presence of gyrotatic microorganisms and Joule heating. Heliyon, 9(8): e18028. https://doi.org/10.1016/j.heliyon.2023.e18028 **PMid:37664738 PMCid:PMC10469572**

Anjum N, Khan WA, Azam M, Ali M, Waqas M, and Hussain I (2023). Significance of bioconvection analysis for thermally stratified 3D Cross nanofluid flow with gyrotactic microorganisms and activation energy aspects. Thermal Science and Engineering Progress, 38: 101596. https://doi.org/10.1016/j.tsep.2022.101596

Bhatti MM, Al-Khaled K, Khan SU, Chammam W, and Awais M (2023). Darcy–Forchheimer higher-order slip flow of Eyring–Powell nanofluid with nonlinear thermal radiation and bioconvection phenomenon. Journal of Dispersion Science and Technology, 44(2): 225-235. https://doi.org/10.1080/01932691.2021.1942035

Dharmaiah G, Dinarvand S, Prasad JR, Noeiaghdam S, and Abdollahzadeh M (2023). Non-homogeneous two-component Buongiorno model for nanofluid flow toward Howarth's wavy cylinder with activation energy. Results in Engineering, 17: 100879. https://doi.org/10.1016/j.rineng.2023.100879

Eid MR, Jamshed W, Goud BS, Ibrahim RW, El Din SM, Abd-Elmonem A, and Abdalla NSE (2023). Mathematical analysis for energy transfer of micropolar magnetic viscous nanofluid flow on permeable inclined surface and Dufour impact. Case Studies in Thermal Engineering, 49: 103296. https://doi.org/10.1016/j.csite.2023.103296

Gangadhar K, Victoria EM, and Chamkha AJ (2024). Effect of entropy minimization and melting heat on gold-magnesium oxide hybrid nanofluid in squeezing channel with magnetic field with radiation. International Journal of Modern Physics B, 38(14): 2450172. https://doi.org/10.1142/S0217979224501728

Ghachem K, Ahmad B, Noor S, Abbas T, Khan SU, Anjum S, Alwadai N, and Kolsi L (2023). Numerical simulations for radiated bioconvection flow of nanoparticles with viscous dissipation and exponential heat source. Journal of the Indian Chemical Society, 100(1): 100828. https://doi.org/10.1016/j.jics.2022.100828

Haq F, Rahman MU, Khan MI, Abdullaeva BS, and Altuijri R (2023). Mathematical modeling and theoretical analysis of bioconvective magnetized sutterby nanofluid flow over rotating disk with activation energy. BioNanoScience, 13(4): 1849-1862. https://doi.org/10.1007/s12668-023-01166-2

Hosseinzadeh K, Mardani MR, Paikar M, Hasibi A, Tavangar T, Nimafar M, Ganji DD, and Shafii MB (2023). Investigation of second grade viscoelastic non-Newtonian nanofluid flow on the curve stretching surface in presence of MHD. Results in Engineering, 17: 100838. https://doi.org/10.1016/j.rineng.2022.100838

Hussain Z, Khan WA, Ali M, Waqas M, and Ashraf IM (2023). Chemically reactive magneto-bioconvection 3D flow of radiative Williamson nanofluid containing oxytactic moment of microorganisms. Tribology International, 189: 108934. https://doi.org/10.1016/j.triboint.2023.108934

Jabeen K, Mushtaq M, Mushtaq T, and Muntazir RMA (2024). A numerical study of boundary layer flow of Williamson nanofluid in the presence of viscous dissipation, bioconvection, and activation energy. Numerical Heat Transfer, Part A: Applications, 85(3): 378-399. https://doi.org/10.1080/10407782.2023.2187494

Jalili P, Narimisa H, Jalili B, Shateri A, and Ganji DD (2023). A novel analytical approach to micro-polar nanofluid thermal analysis in the presence of thermophoresis, Brownian motion and Hall currents. Soft Computing, 27(2): 677-689. https://doi.org/10.1007/s00500-022-07643-2

Javaid M, Tahir M, Imran M, Baleanu D, Akgül A, and Imran MA (2022). Unsteady flow of fractional Burgers' fluid in a rotating annulus region with power law kernel. Alexandria Engineering Journal, 61(1): 17-27. https://doi.org/10.1016/j.aej.2021.04.106

Khan SA, Hayat T, and Alsaedi A (2023). Bioconvection entropy optimized flow of Reiner-Rivlin nanoliquid with motile microorganisms. Alexandria Engineering Journal, 79: 81-92. https://doi.org/10.1016/j.aej.2023.07.069

Khan SU and Shehzad SA (2020). Electrical MHD Carreau nanofluid over porous oscillatory stretching surface with variable thermal conductivity: Applications of thermal extrusion system. Physica A: Statistical Mechanics and its Applications, 550: 124132. https://doi.org/10.1016/j.physa.2020.124132

Li S, Ali F, Zaib A, Loganathan K, Eldin SM, Ijaz Khan M (2023a). Bioconvection effect in the Carreau nanofluid with Cattaneo–Christov heat flux using stagnation point flow in the entropy generation: Micromachines level study. Open Physics, 21(1): 20220228. https://doi.org/10.1515/phys-2022-0228

Li Y, Majeed A, Ijaz N, Barghout K, Ali MR, Muhammad T (2023b). Melting thermal transportation in bioconvection Casson nanofluid flow over a nonlinear surface with motile microorganism: Application in bioprocessing thermal engineering. Case Studies in Thermal Engineering, 49: 103285. https://doi.org/10.1016/j.csite.2023.103285

Maatoug S, Khan SU, Abbas T, Haq EU, Ghachem K, Kolsi L, and Abbasi A (2023). A lubricated stagnation point flow of nanofluid with heat and mass transfer phenomenon: Significance to hydraulic systems. Journal of the Indian Chemical Society, 100(1): 100825. https://doi.org/10.1016/j.jics.2022.100825

Mabood F, Khan SU, and Tlili I (2020). Numerical simulations for swimming of gyrotactic microorganisms with Williamson nanofluid featuring Wu's slip, activation energy and variable thermal conductivity. Applied Nanoscience, 13: 131–144. https://doi.org/10.1007/s13204-020-01548-y

Mebarek-Oudina F and Chabani I (2023). Review on nano enhanced PCMs: insight on nePCM application in thermal management/storage systems. Energies, 16(3): 1066. https://doi.org/10.3390/en16031066

Patil PM, Goudar B, and Momoniat E (2023). Magnetized bioconvective micropolar nanofluid flow over a wedge in the presence of oxytactic microorganisms. Case Studies in Thermal Engineering, 49: 103284. https://doi.org/10.1016/j.csite.2023.103284

Rafique K, Mahmood Z, and Khan U (2023). Mathematical analysis of MHD hybrid nanofluid flow with variable viscosity and slip conditions over a stretching surface. Materials Today Communications, 36: 106692. https://doi.org/10.1016/j.mtcomm.2023.106692

Shamshuddin MD, Shahzad F, Jamshed W, Bég OA, Eid MR, and Bég TA (2023). Thermo-solutal stratification and chemical reaction effects on radiative magnetized nanofluid flow along an exponentially stretching sensor plate: Computational analysis. Journal of Magnetism and Magnetic Materials, 565: 170286. https://doi.org/10.1016/j.jmmm.2022.170286

Sharma BK, Kumawat C, and Bhatti MM (2023a). Optimizing energy generation in power-law nanofluid flow through curved arteries with gold nanoparticles. Numerical Heat Transfer, Part A: Applications, 85(18): 3058–3090. https://doi.org/10.1080/10407782.2023.2232123

Sharma BK, Sharma P, Mishra NK, Noeiaghdam S, and Fernandez-Gamiz U (2023b). Bayesian regularization networks for micropolar ternary hybrid nanofluid flow of blood with homogeneous and heterogeneous reactions: Entropy generation optimization. Alexandria Engineering Journal, 77: 127-148. https://doi.org/10.1016/j.aej.2023.06.080

Sheikholeslami M, Khalili Z, Scardi P, and Ataollahi N (2023). Concentrated solar photovoltaic cell equipped with thermoelectric layer in presence of nanofluid flow within porous heat sink: Impact of dust accumulation. Sustainable Cities and Society, 98: 104866. https://doi.org/10.1016/j.scs.2023.104866

Zheng LC, Jin X, Zhang XX, and Zhang JH (2013). Unsteady heat and mass transfer in MHD flow over an oscillatory stretching surface with Soret and Dufour effects. Acta Mechanica Sinica, 29(5): 667-675. https://doi.org/10.1007/s10409-013-0066-6